Icarus 320 (2019) 7–23

Contents lists available at ScienceDirect

Icarus

journal homepage: www.elsevier.com/locate/icarus

Ceres' Occator crater and its faculae explored through geologic mapping

Jennifer E.C. Scully[a,*], Debra L. Buczkowski[b], Carol A. Raymond[a], Timothy Bowling[c], David A. Williams[d], Adrian Neesemann[e], Paul M. Schenk[f], Julie C. Castillo-Rogez[a], Christopher T. Russell[g]

[a] Jet Propulsion Laboratory, California Institute of Technology, 4800 Oak Grove Drive, Pasadena, CA 91109, USA
[b] Johns Hopkins University Applied Physics Laboratory, Laurel, MD 20723, USA
[c] Southwest Research Institute, Boulder, CO 80302, USA
[d] Arizona State University, Tempe, AZ 85004, USA
[e] Free University of Berlin, 14195 Berlin, Germany
[f] Lunar and Planetary Institute, Houston, TX 77058, USA
[g] University of California, Los Angeles, CA 90095, USA

ARTICLE INFO

Article history:
Received 17 October 2017
Revised 6 April 2018
Accepted 15 April 2018
Available online 20 April 2018

ABSTRACT

Occator crater is one of the most recognizable features on Ceres because of its interior bright regions, which are called the Cerealia Facula and Vinalia Faculae. Here we use high-resolution images from Dawn (~35 m/pixel) to create a detailed geologic map that focuses on the interior of Occator crater and its ejecta. Occator's asymmetric ejecta indicates that the Occator-forming impactor originated from the northwest at an angle of ~30–45°, perhaps closer to ~30° Some of Occator's geologic units are analogous to the units of other complex craters in the region: the ejecta, crater terrace material, hummocky crater floor material and talus material. The geologic units that make Occator unique are the bright Occator pit/fracture material (this is the unit that corresponds to the Cerealia Facula and Vinalia Faculae) and the extensive, well-preserved lobate materials. We propose that the lobate materials are a slurry of impact-melted and non-impact-melted target material, which flowed around the crater interior before solidifying to form deposits geomorphologically consistent with impact melts elsewhere in the Solar System. We sub-divide the lobate materials on the basis of their surface textures. It is likely that knobby or smooth lobate materials form if the lobate material entrains or does not entrain blocks, respectively. Post-impact inflation is suggested to form the hummocky lobate material. The Vinalia Faculae formed within the hummocky lobate material. We find that the knobby lobate material and the outer edge of the Cerealia Facula formed prior to the central pit. The central dome formed after the formation of the central pit, while the majority of the Cerealia Facula (besides the outer edge) could have formed, continued to form and/or have been modified after the formation of the central pit. The Cerealia Facula may have initially been emplaced in a similar process to the Vinalia Faculae, and the surface of the Cerealia Facula appear to have somewhat darkened over time. The insights into Occator crater and its faculae derived from our geologic mapping will be synthesized together with inputs from all of the studies in this special issue in Scully et al. (2018a).

1. Introduction

Ceres was first explored from orbit by the Dawn mission, which reached the dwarf planet in March 2015. Ceres is the only dwarf planet located in the inner solar system and is the largest object in the asteroid belt, with triaxial elliptical dimensions of 483.1 ± 0.2 km, 481.0 ± 0.2 km and 445.9 ± 0.2 km (Russell et al., 2016). Dawn has explored Ceres using its Framing Camera (FC) (Sierks et al., 2011), Visible-Infrared Mapping Spectrometer (VIR) (De Sanctis et al., 2011), Gamma Ray and Neutron Detector (GRaND) (Prettyman et al., 2011), and gravity science investigation (Konopliv et al., 2011). Dawn data confirms that Ceres is partially differentiated into a rocky interior and a more volatile-rich outer layer (Park et al., 2016; Russell et al., 2016), which is on average $41.0^{+3.2}_{-4.7}$ km thick, based on a dynamic isostasy model

* Corresponding author.
E-mail address: jennifer.e.scully@jpl.nasa.gov (J.E.C. Scully).

https://doi.org/10.1016/j.icarus.2018.04.014
0019-1035/

(Ermakov et al., 2017a). The outer layer is a mixture of phyllosilicates and/or carbonates, salts and/or clathrate hydrates and < 30–40% water ice by volume (Bland et al., 2016; Fu et al., 2017; Hiesinger et al., 2016). Mass wasting has exposed water ice on the surface (e.g. Combe et al., 2016; Hughson et al., 2018), sputtering of near-surface water ice is interpreted to form a transient atmosphere (Villarreal et al., 2017), and surficial water ice is thought to occur in permanently shadowed craters (Ermakov et al., 2017b; Schorghofer et al., 2016; Platz et al., 2016). Water ice and/or volatiles are interpreted to be involved in the formation of domical features, pitted terrain and lobate flows (Buczkowski et al., 2016; Ruesch et al., 2016; Schmidt et al., 2017; Sizemore et al., 2017). The surface has a relatively low average single scattering albedo of 0.09–0.11 (Li et al., 2016) and is composed of a mixture of ammonia-bearing phyllosilicates, magnesium-bearing phyllosilicates, carbonates and a dark component (De Sanctis et al., 2015). There are ~500 impact craters > 20 km in diameter spread across the surface, and both simple and complex crater morphologies are present (Buczkowski et al., 2016; Marchi et al., 2016). The transition from simple craters to complex craters occurs at a diameter of ~7.5–12 km (Hiesinger et al., 2016). For more details about Ceres and Dawn's exploration, see Scully et al. (2018b).

Occator crater is located in Ceres' northern hemisphere (20 °N, 239 °E), is a complex crater and is ~92 km in diameter (Fig. 1a). It is one of the most intriguing and recognizable features on Ceres' surface because it contains regions in its floor, called faculae, that are much brighter than Ceres' average: a single scattering albedo of 0.67–0.80 versus 0.09–0.11 (Li et al., 2016). Moreover, the average visual normal albedo of the faculae is six times Ceres' average (Schröder et al., 2017). The central region is called the Cerealia Facula and the faculae in the eastern crater floor are called the Vinalia Faculae (Fig. 1b). There is a ~9 km wide and ~800 m deep central pit within the crater, which contains Cerealia Facula and a ~300–700 m high central dome (Schenk et al., 2016; Nathues et al., 2015). While the majority of Ceres' surface has a uniform composition (Ammannito et al., 2016), Occator's faculae are mostly composed of sodium carbonate (De Sanctis et al., 2016). In addition to the faculae, there are also extensive lobate materials within Occator's floor (Fig. 1b), which have been proposed to be impact melt, or mass wasting deposits from crater-wall collapse, or cryovolcanic flows (e.g. Jaumann et al., 2017; Krohn et al., 2016; Nathues et al., 2017; Schenk et al., 2016).

Occator crater was mapped as a part of the Dawn team's global mapping project, during which the surface of Ceres was divided into fifteen regions, called quadrangles (Williams et al., 2018). Occator crater is located on the border of two of these quadrangles: the larger portion of the crater is located within Occator quadrangle (Buczkowski et al., 2018a) while the smaller portion is located within Ezinu quadrangle (Scully et al., 2018c). Occator crater was included in both of these quadrangle maps, which are displayed at a scale of 1:1,000,000. These maps illustrate the broad-scale geologic units and features within Occator crater. However, minimum dimension criteria were applied, which resulted in the omission of small-scale details. For example, geologic units that are < 5 km wide and linear features that are < 5 km long or spaced at < 3 km were not included in the quadrangle maps.

Here we present a detailed map of the interior of Occator crater and its ejecta. There are no minimum dimension criteria applied throughout this map. However, the scale of the features that can be mapped is limited by the resolution of the basemap (~35 m/pixel) (see Section 2.1.1). The aim of this focused and detailed mapping is to provide new insights into Occator and its faculae. These insights can, in turn, be combined with additional studies to illuminate the driving forces behind the formation and evolution of Occator and its faculae (Scully et al., 2018a). Whether the driving forces behind the faculae's formation are entirely impact-derived/exogenic, entirely endogenic or a combination of both will lead to a new understanding of the processes and conditions in Ceres' past, and potentially in its present. For further details about our motivation for studying Occator crater and its faculae, see Scully et al. (2018b).

2. Methods: geologic mapping

2.1. Data sources

2.1.1. Basemap

Dawn returned data from Ceres during four orbital stages of decreasing altitude: Approach (> 4400 km), Survey (4400 km), High Altitude Mapping Orbit (HAMO, 1470 km) and Low Altitude Mapping Orbit (LAMO, 385 km). The basemap upon which we based our geologic map of Occator crater is a mosaic of clear filter Framing Camera LAMO images (~35 m/pixel), made by the German Aerospace Center (DLR) (Fig. 2) (Roatsch et al., 2017). The clear filter's panchromatic images have a wavelength range of 450–920 nm (Sierks et al., 2011). Due to the large brightness contrast between the faculae and the other materials in Occator crater, we displayed the mosaic of the data (in reflectance values) with different stretches in ArcMap 10.3 software, which we used for our mapping (see Section 2.2). A standard deviation stretch with $n = 10$ is appropriate for mapping the majority of the crater and its ejecta. A standard deviation stretch with $n = 27$ highlights the details of the faculae. A standard deviation stretch with $n = 60$ emphasizes brighter regions within the faculae (Fig. 2a i–iii).

2.1.2. Supplementary datasets

While we use the LAMO basemap to define the mapped features, we also use supplementary datasets to assist with our analysis of these features:

- We use two shape models of Occator crater, both of which are produced from clear filter Framing Camera LAMO images. One is produced using the stereophotogrammetry (SPG) technique by DLR (Fig. S1a) (Jaumann et al., 2017) and one is produced using the stereophotoclinometry (SPC) technique by JPL (Fig. S1b). The SPG shape model has a lateral grid spacing of ~32 m/pixel, a mean intersection error of +/−2.8 m, an intrinsic height accuracy of ~1.5 m and is referenced to a 470 km sphere. The SPC shape model has a horizontal resolution of ~800 m/pixel, a vertical accuracy/absolute radial error of > 20 m and is referenced to an ellipsoid with axes of 482,147 m and 445,930 m (Park et al., 2016). A SPC shape model with a horizontal resolution of ~100 m/pixel is now available, but was not used during the time of our analysis. In order to compare the relative elevations between features, we use these shape models in flat, plan views and we also use them to create profiles. While the absolute values of elevation vary between the two shape models, the relative elevation differences between features are consistent between both shape models. We also use perspective views with no vertical exaggeration, which are made by overlaying Framing Camera clear filter LAMO images onto the SPG shape model of Occator (created by David P. O'Brien, Planetary Science Institute).
- Anaglyphs of parts of Occator crater also allow us to view the crater in three dimensions (Fig. S2). These anaglyphs are made from the clear filter Framing Camera LAMO images (~35 m/pixel) by Thomas Platz (Max Planck Institute for Solar System Research).
- The photometrically corrected mosaic of clear filter Framing Camera HAMO images, produced by DLR (~140 m/pixel), allows us to interpret whether the dark or bright appearance of regions in the basemap is controlled by their intrinsic brightness or by the solar illumination conditions under which they were

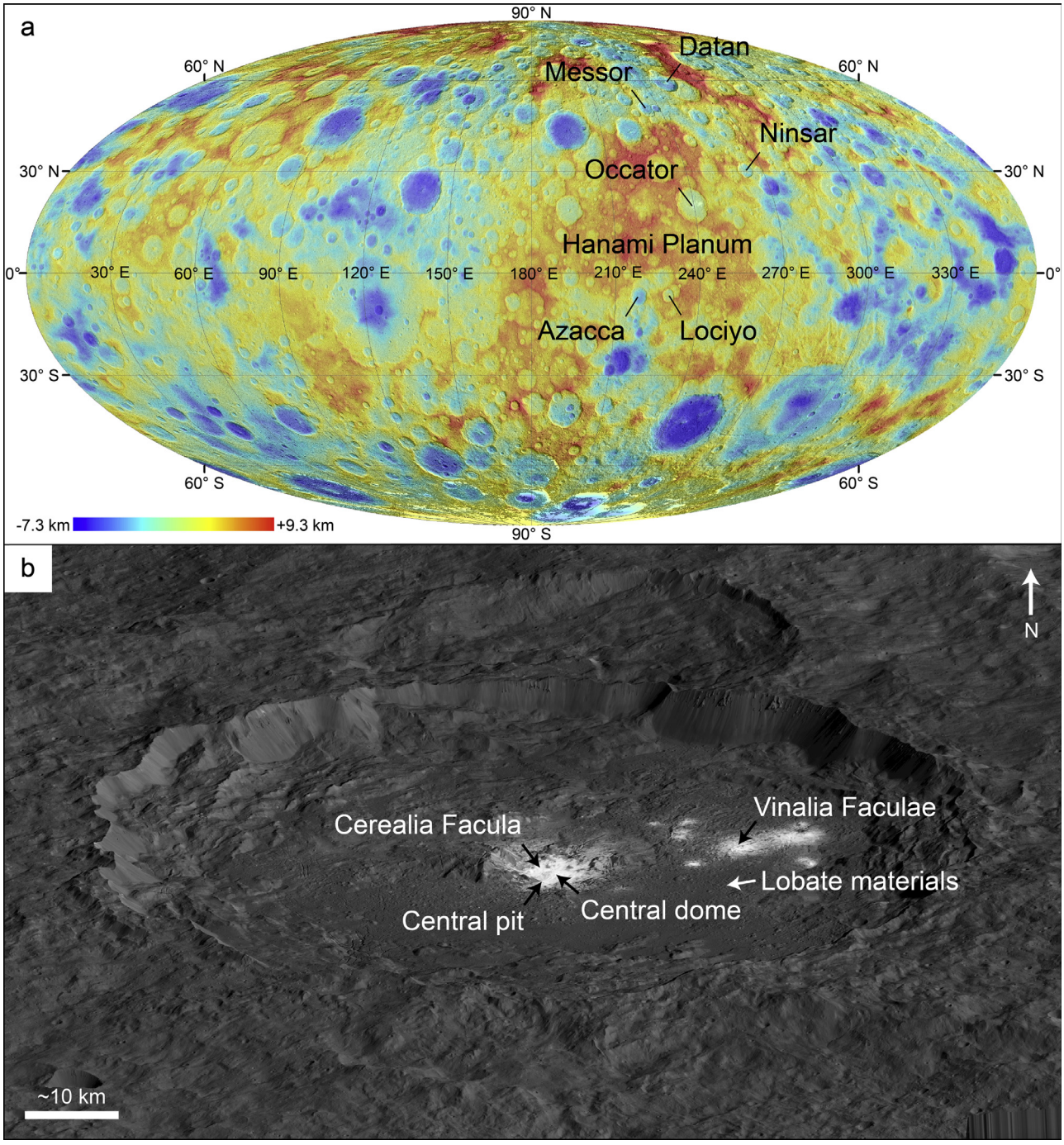

Fig. 1. (a) The location of Occator crater on the global shape model of Ceres, which is overlain onto a global LAMO (Low Altitude Mapping Orbit) mosaic, in a Mollweide projection. Hanami Planum and craters mentioned in the text are also labeled. This HAMO-based (High Altitude Mapping Orbit), global shape model is provided by DLR, is referenced to a 482 × 446 km biaxial ellipsoid and has a lateral spacing of 60 pixels per degree, corresponding to ~135 m/pixel and a vertical resolution of <100 m (Preusker et al., 2016). The global LAMO mosaic of clear filter Framing Camera images (~35 m/pixel) is made by the German Aerospace Center (DLR). (b) Perspective view of Occator crater, with the Cerealia Facula, Vinalia Faculae, central pit, central dome and lobate materials indicated. The view has no vertical exaggeration and was made by David P. O'Brien (Planetary Science Institute).

observed (Fig. S3). The geologic units we map have intermediate brightness in the photometrically corrected data. When necessary, we sub-divide each geologic unit into dark or bright categories if they are distinctly dark or bright in the photometrically corrected data. We define a sub-unit as dark, intermediate or bright with reference to their pixel values, which are included for each unit in Section 3.2. Methods by which Framing Camera data can be photometrically corrected are outlined in Schröder et al. (2017).

2.2. Mapping approach

We define our map area to extend from the center of Occator crater to the farthest mapped extent of its ejecta blanket. To map the crater, we used ESRI ArcMap 10.3 software, which allowed us to georeference our mapping to the datasets and to measure the length, area, etc. of the mapped features. Using ArcMap we viewed the basemap, the shape models, the anaglyphs and the photometrically corrected data in plan view. We used the spatial analyst tool-

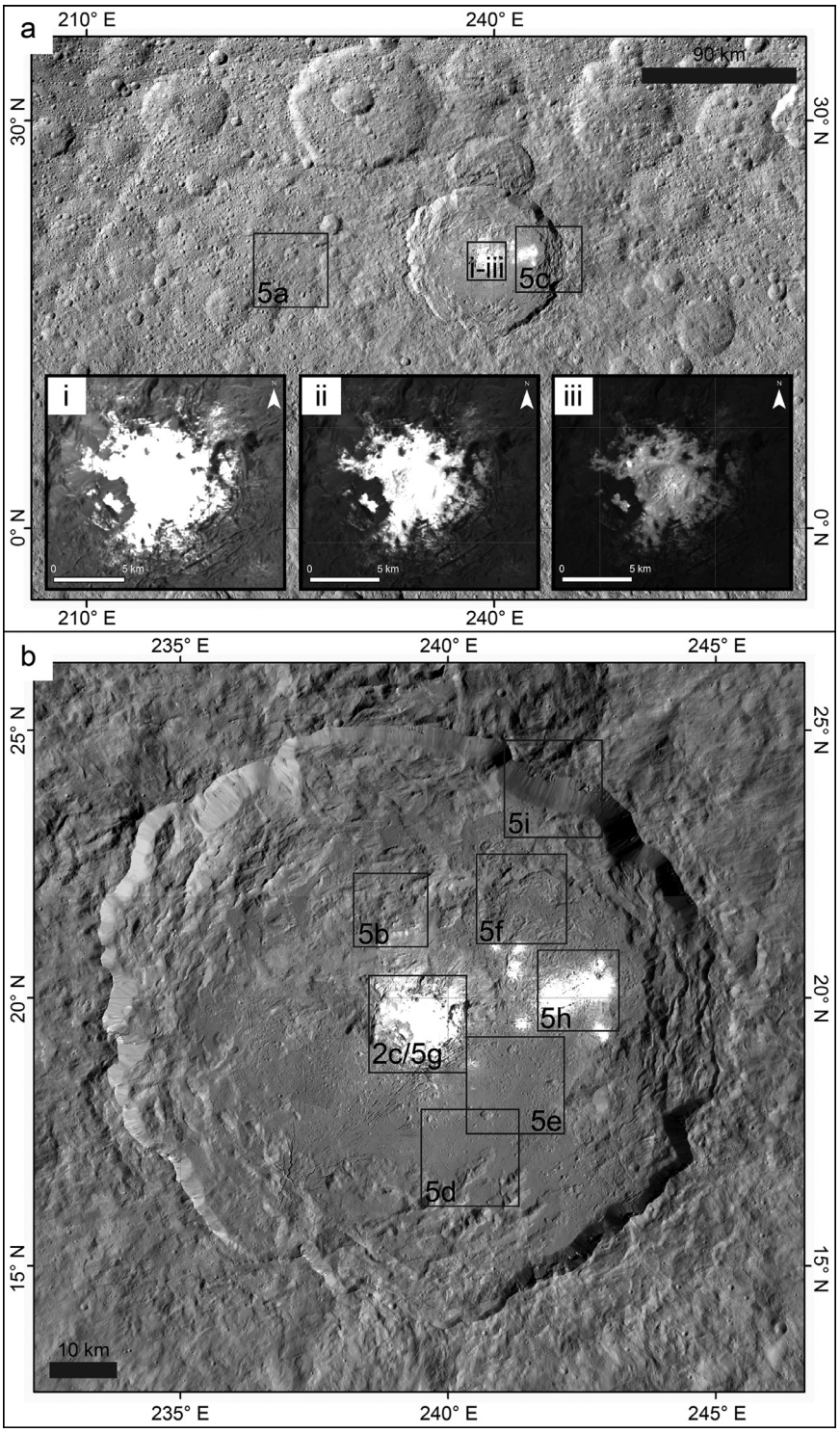

Fig. 2. (a) The basemap for our geologic map of Occator crater is a mosaic of clear filter Framing Camera LAMO images (~35 m/pixel), made by the German Aerospace Center (DLR) (Roatsch et al., 2017). The inset figures (i–iii) illustrate the appearance of Cerealia Facula with a standard deviation stretch of $n = 10$, $n = 27$ and $n = 60$ respectively. (b) The interior of Occator crater, as it appears in our basemap. In both (a) and (b), the locations of the nine parts of Fig. 5 are illustrated. Both (a) and (b) are displayed with an equirectangular projection, in which the scale bar is valid at the equator and the distortion increases towards the poles.

bar in ArcMap to create profiles from the plan view of the shape models. We viewed the perspective views separately, but alongside, the data in ArcMap.

The resolution of our basemap facilitated mapping at a scale of 1:100,000. We mapped all features that were identifiable at this scale and did not use minimum dimension criteria. The smallest mapped geologic unit is ~600 m in its longest dimension. Here we display the entire geologic map with a reference scale of 1:1,500,000 (Fig. 3a), the geologic map of the interior of Occator crater with a reference scale of 1:500,000 (Fig. 4) and the geologic map of the center of Occator crater with a reference scale of 1:250,000 (Fig. 3b). The legend in Fig. 4 applies to all

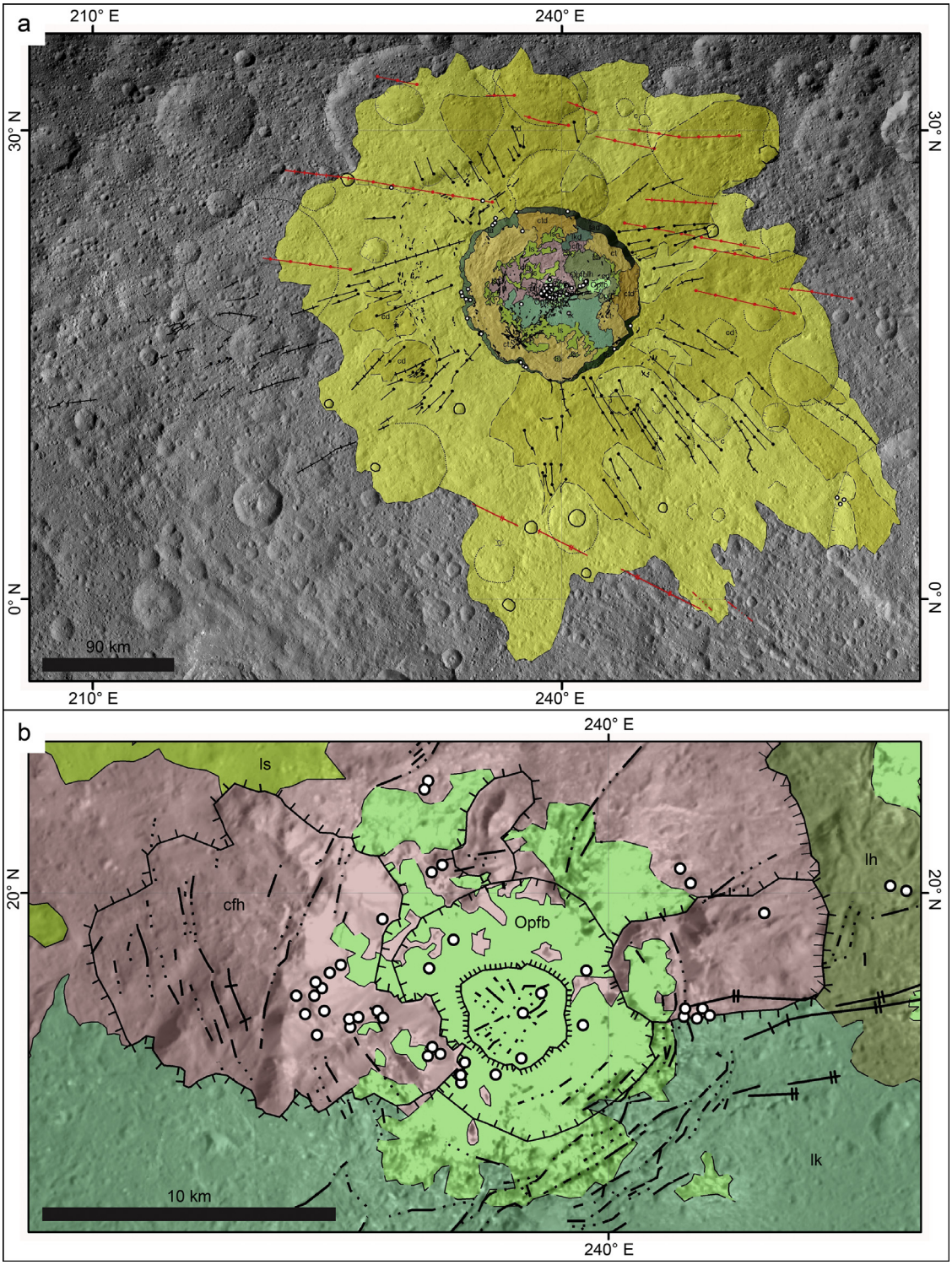

Fig. 3. (a) Our entire geologic map of Occator crater and its ejecta, which is overlain onto the basemap. This map was created by mapping at a scale of 1:100,000, but is shown with a reference scale of 1:1,500,000 to make the symbols more legible in publication format. The legend is included in Fig. 4. The map is displayed with an equirectangular projection, in which the scale bar is valid at the equator and the distortion increases towards the poles. (b) Our geologic map of the center of Occator crater, which is overlain onto the basemap. This map was created by mapping at a scale of 1:100,000, but is shown with a reference scale of 1:250,000 to make the symbols more legible in publication format. The legend is included in Fig. 4. A high-resolution version of this figure is included in the supplementary material (Fig. S4).

of these maps. High-resolution versions of each of these geologic maps are available in the supplementary material (Fig. S4 and Fig. S5). Following the Dawn science team's practice of consulting the United States Geological Survey (USGS) guidelines during the production of the quadrangle maps (Williams et al., 2018), we mainly used map symbols based on the standardized symbology recommended by the USGS for planetary geologic features (Federal Geographic Data Committee, 2006).

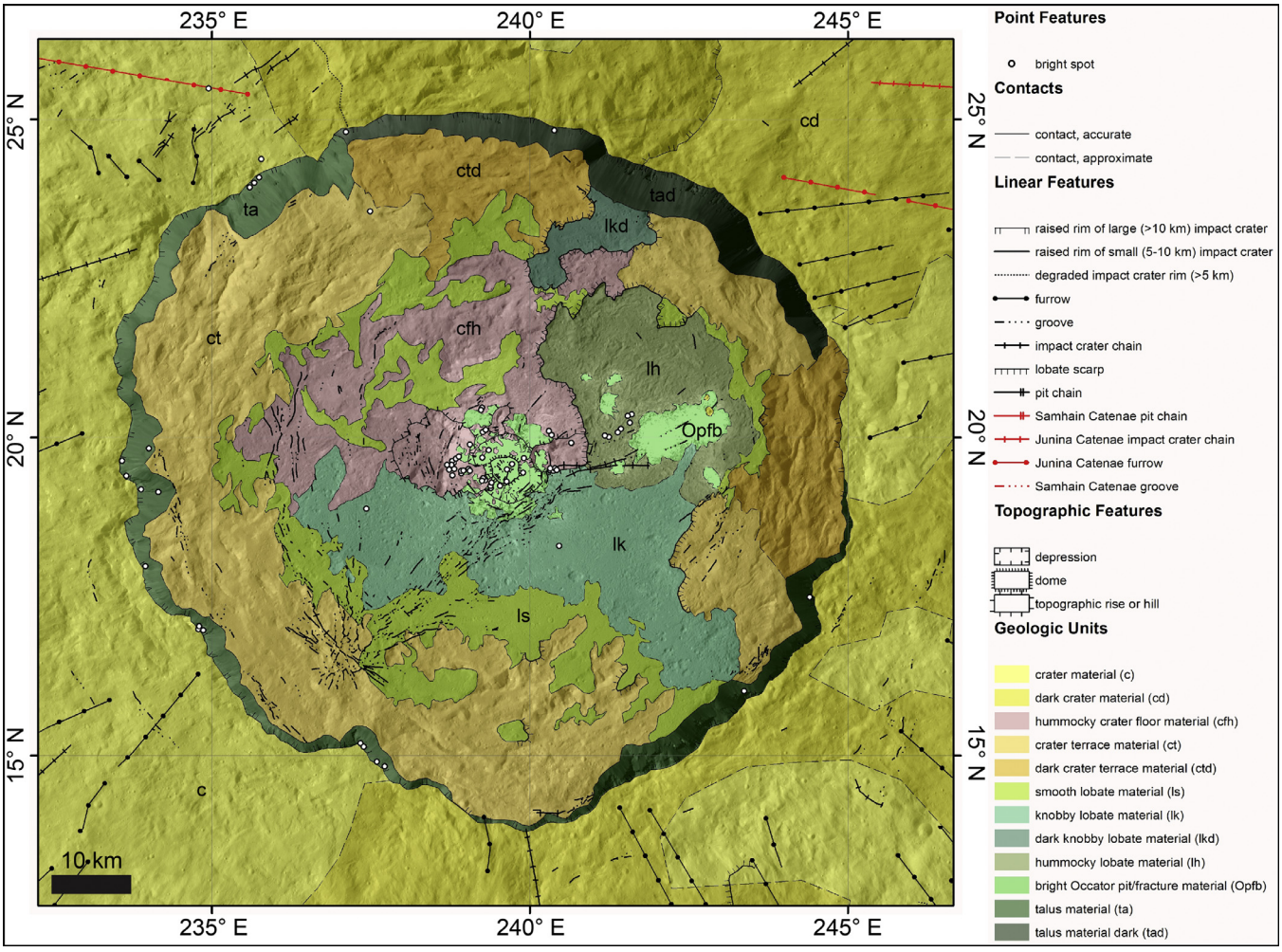

Fig. 4. Our geologic map of the interior of Occator crater, which is overlain onto the basemap. This map was created by mapping at a scale of 1:100,000, but is shown with a reference scale of 1:500,000 to make the symbols more legible in publication format. The legend is for all of the mapped features and also applies to Fig. 3. The map is displayed with an equirectangular projection, in which the scale bar is valid at the equator and the distortion increases towards the poles. A high-resolution version of this figure is included in the supplementary material (Fig. S5).

3. Results

3.1. Regional setting of Occator crater

Occator crater is located within a region called Hanami Planum (Fig. 1a). This region is ~500 km wide, is topographically high and has the strongest negative Bouguer anomaly on Ceres. This could be explained by an underlying buoyancy-driven anomaly and high rigidity/thick outer layer or by a relatively low regional density (Ermakov et al., 2017a). To Occator's north, within Ezinu quadrangle, the ancient cratered terrain dominates the surface (~3–4 billion years old) (Scully et al., 2018c). Some complex impact craters have ejecta blankets that superpose the cratered terrain: Ninsar (40 km diameter), Datan (60 km diameter) and Messor (40 km diameter) (Fig. 1a). These impact craters are young (a few hundreds of millions of years) in comparison to the cratered terrain, and their interiors contain crater terrace material and hummocky crater floor material, which are interpreted to form by collapse and mass wasting shortly following the craters' formation (Scully et al., 2018c). More recent mass wasting has covered the walls of these craters with talus material. Complex craters of a similar age are also found to Occator's south: Azacca (50 km diameter) and Lociyo (38 km diameter) (Fig. 1a). These craters are also surrounded by ejecta blankets and contain crater terrace material, hummocky crater floor material and talus material (Buczkowski et al., 2018a), which often have different spectral properties than the surrounding cratered terrain (Longobardo et al., 2018). For example, Azacca crater and its ejecta contain sodium carbonate (Carrozzo et al., 2018).

3.2. Description of map units

In the following subsections we discuss our observations and interpretations of each geologic unit in our geologic map (Fig. 3 and Fig. 4). In Table 1, we list the symbols and RGB colors of each of these units.

3.2.1. Crater material, dark crater material

Observations: The majority of this unit is located around Occator crater, mostly to the southeast. The crater material surrounding Occator superposes the cratered terrain and contains less impact craters than the cratered terrain, which give it a comparatively smoother texture (Fig. 5a) (Scully et al., 2018c). The boundaries between the crater material and the cratered terrain are mapped with approximate contacts because the exact locations of the boundaries between the two units are not usually visible. The dark crater material sub-unit is distinctly dark (pixel value: 0.01–0.05) in the photometrically corrected data, in comparison to the

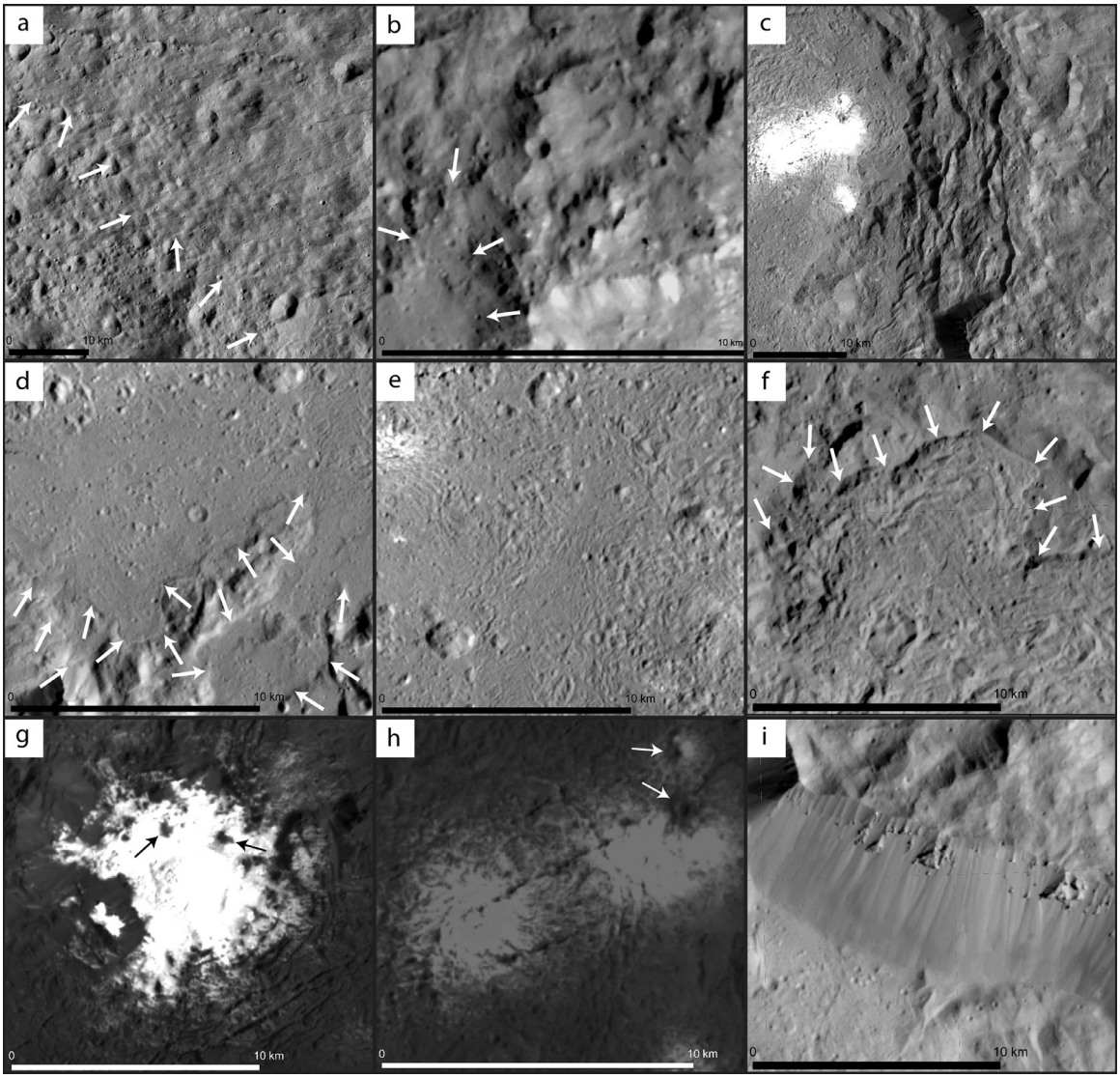

Fig. 5. The type areas for each of the geologic units in our geologic map, as they appear in the basemap. Each scale bar represents 10 km. The location of each panel is indicated in Fig. 2 and north is up in all panels. (a) Crater material: the white arrows indicate the margin of the crater material, which superposes the cratered terrain (located in bottom left of the frame). (b) The hummocky crater floor material fills the entire frame apart from a region of smooth lobate material, which is outlined by white arrows. (c) The crater terrace material is located from the top to the bottom of the center of the frame. (d) The smooth lobate material fills the entire frame apart from a region of crater terrace material in the bottom of the frame. The boundary between these two units is indicated by the white arrows. The smooth lobate material begins to transition into knobby lobate material at the top of the frame. (e) The knobby lobate material fills the entire frame. (f) The hummocky lobate material, whose northern boundary is indicated by the white arrows. (g) The Cerealia Facula portion of the bright Occator pit/fracture material, which is located in the center of the frame. The black arrows indicate the two small regions of hummocky crater floor material within Cerealia Facula. (h) The Vinalia Faculae portion of the bright Occator pit/fracture material, which is located in the center of the frame. The white arrows indicate the two small impact craters and their dark ejecta blankets, which superpose part of the Vinalia Faculae. (i) The talus material, which is located in the middle of the frame and fills the entire crater wall.

Table 1
The symbols and RGB colors for each of the geologic units within our map (Figs. 3 and 4). The units are displayed with a transparency of 50%.

Unit name	Symbol on map	RGB color on map
Crater material	c	255-255-51
Dark crater material	cd	240-230-0
Hummocky crater floor material	cfh	217-149-148
Crater terrace material	ct	255-206-51
Dark crater terrace material	ctd	242-174-0
Smooth lobate material	ls	164-222-0
Knobby lobate material	lk	73-195-134
Dark knobby lobate material	lkd	45-125-90
Hummocky lobate material	lh	122-152-62
Bright Occator pit/fracture material	opfb	51-204-51
Talus material	ta	0-76-0
Dark talus material	tad	0-40-0

intermediate brightness of the crater material (pixel value: 0.05–0.06). The dark crater material superposes the crater material and is mostly located on the eastern side of Occator (Fig. 3 and Fig. S3a). The exact location of the boundaries between the crater material and dark crater material are not visible in the photometrically corrected data, and thus we map them with approximate contacts. We also identify two small regions of dark crater material inside of Occator crater, which surround two small impact craters (a few hundreds of meters in diameter) that superpose the Vinalia Faculae (see Section 3.2.7).

Interpretations: We interpret this unit as ejecta that was formed by material ejected during the formation of Occator crater, and by the small craters that superpose the Vinalia Faculae. It is commonly observed that the order of the layering of ejecta deposits is reversed in comparison to the order of the layering of the

subsurface materials from which the ejecta was excavated. Thus, we interpret that the dark crater material, which in order to be visible must superpose the crater material, was excavated from deeper within Ceres' subsurface than the crater material. The concentration of the dark crater material on the eastern side of Occator could be explained by the inhomogeneous distribution of dark source material: the dark source material may be more common within the eastern subsurface or it may be more deeply buried within the western subsurface. See Nathues et al. (2018) and Raponi et al. (2018) for further discussion of the dark crater material.

3.2.2. Hummocky crater floor material

Observations: This unit is located in the northern and western parts of Occator's floor and has an irregular/blocky surface texture, which gives it a hummocky appearance (Fig. 5b). The unit shares certain contacts with the crater terrace material and there is no superposition relationship between them. It has an intermediate brightness in the photometrically corrected data (pixel value: 0.05–0.06).

Interpretations: We interpret this unit as a mass wasting deposit, which infilled the floor as material collapsed from Occator's walls to the floor during/shortly after the formation of the crater. This unit likely formed contemporaneously with the crater terrace material, because neither superposes the other.

3.2.3. Crater terrace material, dark crater terrace material

Observations: The unit forms a ring around the interior of Occator crater and consists of steps, or terraces, which are roughly concentric to the crater rim (Fig. 5c). The only breaks in this ring are in the southeastern and northeastern quadrants of the crater, where the knobby and dark knobby lobate materials superpose the terraces (see Section 3.2.5). The terraces in the southwestern quadrant of the crater are approximately perpendicular to the terraces in the southeastern quadrant, and they converge at a ~90° bend in the crater rim (Fig. 6). The unit shares certain contacts with the hummocky crater floor material and there is no superposition relationship between them. The dark crater terrace material sub-unit is distinctly dark (pixel value: 0.01–0.05) in the photometrically corrected data, in comparison to the intermediate brightness of the crater terrace material (pixel value: 0.05–0.06). The exact location of the boundaries between the crater terrace material and dark crater terrace material are not visible in the photometrically corrected data, and thus we map them with approximate contacts.

Interpretations: We interpret that this unit formed during/shortly after the formation of the crater, as portions of the crater walls collapsed in a coherent fashion to form the stepped, or terraced, morphology. This unit likely formed contemporaneously with the hummocky crater floor material, because neither superposes the other. More recent mass wasting and collapse has also probably occurred on the steeply dipping terraces within this unit. We suggest that the ~90° bend in the southern crater rim was formed when the actively collapsing sets of southwestern and southeastern terraces converged together. There are other smaller scale and more obtuse bends within the crater rim that also likely formed because of the convergence of other sets of roughly perpendicular terraces.

3.2.4. Smooth lobate material

Observations: The lobate materials are located within two regions of Occator crater: (1) they form an extensive deposit that fills the southern and eastern parts of the crater floor and (2) they form separate pond-like deposits at different elevations throughout the crater interior (Fig. 7a). The smooth lobate material is located at the southernmost and easternmost edges of the extensive floor deposit. In the southern part of the extensive floor deposit, the smooth lobate material superposes the crater terrace material and appears to have flowed between the terraces. Pond-like deposits of this unit also superpose the hummocky crater floor material and crater terrace materials at different elevations throughout the crater. These pond-like deposits have distinct, rounded margins in plan view, which we map with certain contacts. This unit has a smooth surface texture that distinguishes it from the other lobate materials (Fig. 5d). We map the margins of the unit as lobate scarps when the unit displays distinct, rounded margins, superposes the substrate and forms an area of localized high topography (few tens to few hundreds of meters). The smooth lobate material transitions into both the knobby and hummocky lobate materials, and thus we classify their shared contacts as approximate. None of the regions of smooth lobate materials display a clear origination point.

Interpretations: We interpret this unit as flows that superpose the underlying units. We discuss the nature of this flow in Section 4.1.3. Underlying, pre-existing pinnacles or other topographic features could disrupt or break the smooth surface of the flow. In order for the surface to remain smooth, the smooth lobate material must be thick enough to bury any pre-existing pinnacles or other topographic features, and/or these features must not be present below the smooth lobate material. However, the smooth lobate material is concentrated next to the terraces, and in ponds that superpose the terraces and hummocky crater floor material, making it more likely to be thinner in comparison to the knobby lobate material (see Section 3.2.5). Thus, the smooth surface texture of this unit may simply indicate that there is a lack of entrained blocks within the flow.

3.2.5. Knobby lobate material, dark knobby lobate material

Observations: The knobby lobate material is located within the extensive floor deposit of lobate materials (Fig. 5e and Fig. 7a). This extensive deposit of lobate materials does not display a clear origination point. The knobby texture of this unit arises from a smooth surface that is interspersed with irregular shaped mounds, which distinguishes it from the other lobate materials. The southeastern region of the knobby lobate material superposes the crater terrace material. The terraces on either side of the knobby lobate material trend in the same direction (Fig. 7b). In the northeastern part of the crater interior, the dark knobby lobate material superposes the hummocky crater floor material and crater terrace material in a sinuous deposit that appears to have flowed inwards. The dark talus material along the crater wall obscures the origination point of the dark knobby lobate material. The dark knobby lobate material sub-unit is distinctly dark (pixel value: 0.01–0.05) in the photometrically corrected data, in comparison to the intermediate brightness of the knobby lobate material (pixel value: 0.05–0.06). The knobby lobate material and dark knobby lobate material share approximate contacts. We map the margins of the unit as lobate scarps when the unit displays distinct, rounded margins, superposes the substrate and forms an area of localized high topography (few tens to few hundreds of meters). The knobby lobate material transitions into both the smooth and hummocky lobate materials, and thus we classify their shared contacts as approximate.

Interpretations: We interpret this unit as flows that superpose the underlying units. We discuss the nature of this flow in Section 4.1.3. In the southeast, the knobby lobate material appears to have flowed out over the center of a set of terraces that were originally connected, because these terraces trend in the same direction on either side of the superposing knobby lobate material (Fig. 7b). Underlying, pre-existing pinnacles or other topographic features could disrupt or break the surface of the flow, forming the knobby texture. In order for this to occur, the knobby lobate material must be thin enough to expose the pre-existing pinnacles or other topographic features, and these features must be present

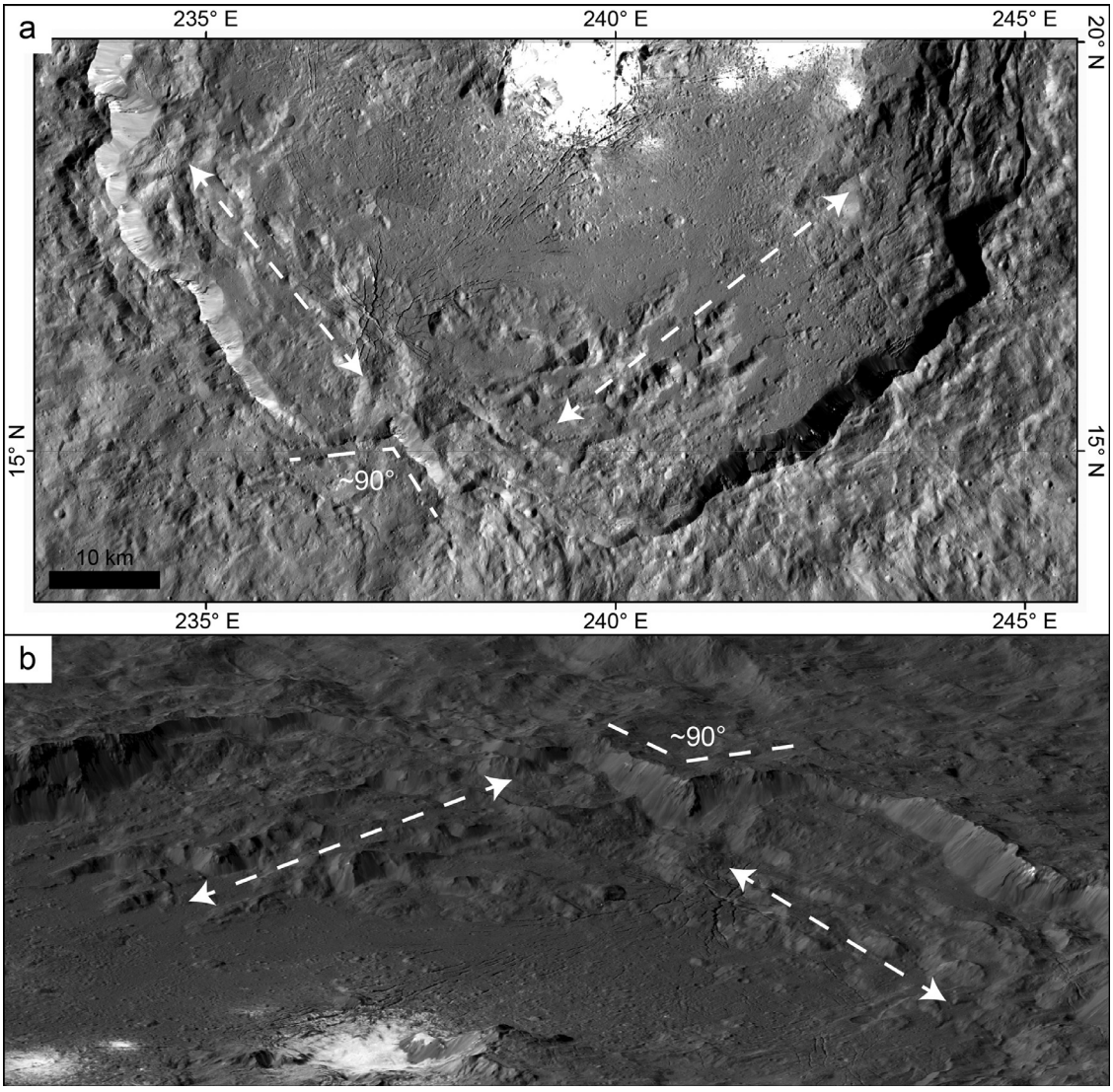

Fig. 6. The terraces in the southwestern and southeastern quadrants of the crater, which are approximately perpendicular to one another and converge at a ~90° bend in the crater rim. The terraces are illustrated in (a) the basemap and (b) in the perspective view, which has no vertical exaggeration and was made by David P. O'Brien (Planetary Science Institute).

below the knobby lobate material. However, the knobby lobate material is mostly located within the center of the crater, making it more likely to be thicker in comparison to the smooth lobate material (see Section 3.2.4). Thus, the knobby surface texture of this unit may simply indicate that it contains entrained blocks.

3.2.6. Hummocky lobate material

Observations: The hummocky lobate material forms the northeastern part of the extensive floor deposit of lobate materials. It superposes the crater terrace material and the hummocky crater floor material. This extensive deposit of lobate materials does not display a clear origination point (Fig. 7a). The hummocky lobate material has an undulating surface composed of sinuous troughs and ridges that are sometimes concentric to the margins of the unit, which distinguishes it from the other lobate materials (Fig. 5f). The unit often displays distinct, rounded margins, superposes the substrate and forms an area of localized high topography (few tens to few hundreds of meters), in which case we map the margins of the unit as lobate scarps. The hummocky lobate material transitions into both the smooth and knobby lobate materials. Thus we classify their shared contacts as approximate.

Interpretations: We interpret this unit as flows that superpose the underlying units. We discuss the nature of this flow in Section 4.1.3. The hummocky texture is suggested to result from post-emplacement modification, such as inflation (Buczkowski et al., 2018b).

3.2.7. Bright occator pit/fracture material

Observations: This unit corresponds to the Cerealia Facula and Vinalia Faculae, which in the photometrically corrected data are distinctly brighter than every other unit within the geologic map (pixel value: >0.06). The majority of Cerealia Facula is a roughly circular continuous deposit of bright material that is almost entirely located within the central pit of Occator crater (see Section 3.5). The majority of Cerealia Facula is partly surrounded by an outer edge that forms a discontinuous halo of more diffuse bright material (Fig. 5g). The outer, diffuse edge of Cerealia Facula tends to concentrate in between the topographic rises that are adjacent to the central pit (Fig. 8). However, it does sometimes extend up parts of the flanks of these topographic rises. These topographic rises may be the remnants of an initial central peak. Cerealia Facula superposes the hummocky crater floor material and the

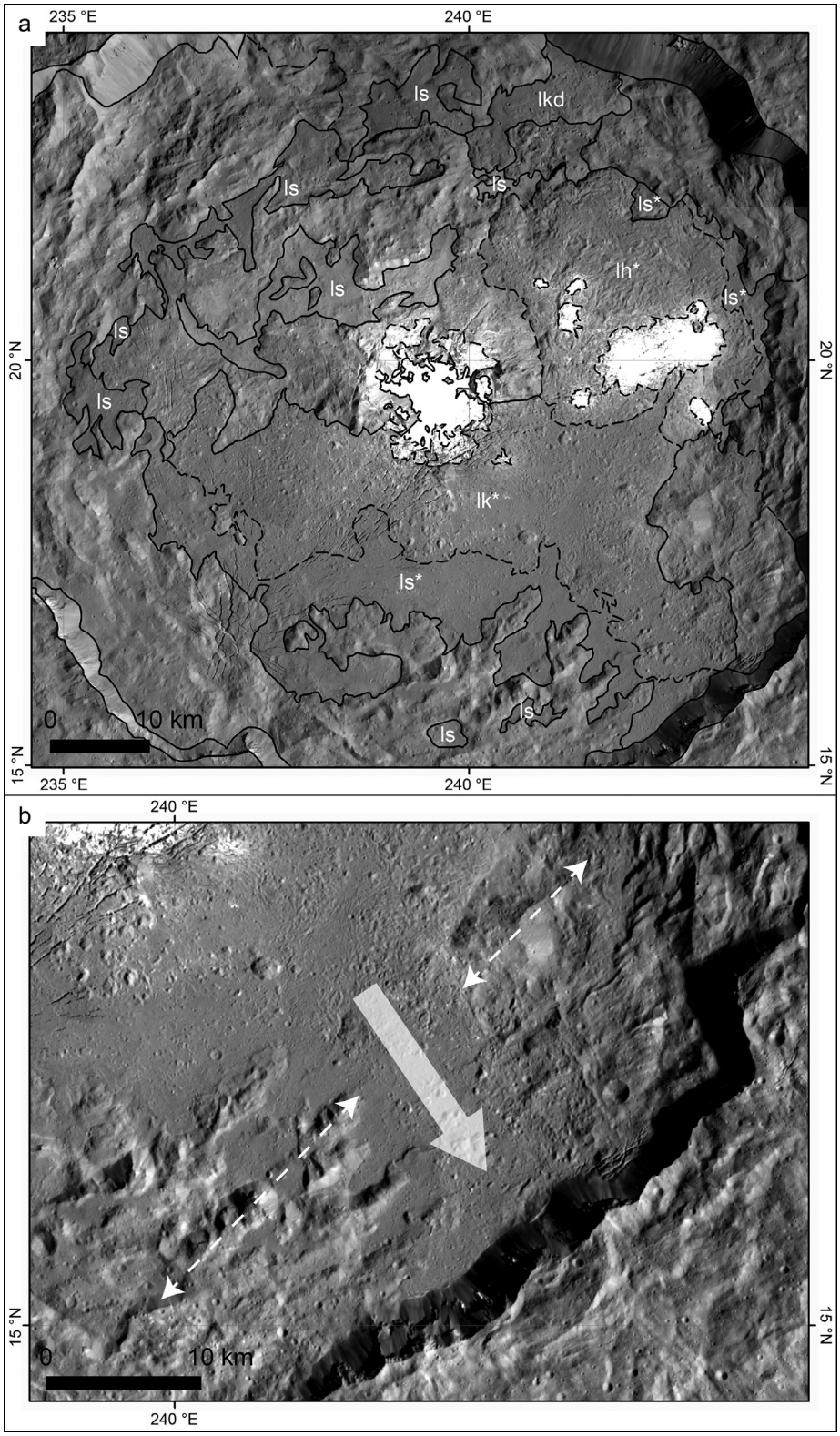

Fig. 7. The lobate materials within Occator crater. (a) The contacts surrounding all mapped regions of the smooth (ls), knobby (lk) and hummocky (lh) lobate materials are shown on the basemap. The mapped regions of lobate materials are similar to those shown in Scully et al. (2018c), but units smaller than the minimum dimension criteria cut-off (< 5 km wide) are shown in this figure. The lobate materials form both an extensive deposit that fills the southern and eastern parts of the crater floor and separate pond-like deposits. The lobate materials that are part of the extensive deposit are labeled with a * and the separate pond-like deposits are not labeled with a *. (b) This figure illustrates a portion of the knobby lobate material that superposes the crater terrace material. The dashed white arrows indicate the similar trend of the terraces on either side of the knobby lobate material. The large white arrow indicates the hypothesized direction of flow of the knobby lobate material over the terraces. There is no source region for this part of the knobby lobate material along the crater rim. There is also no contact between this part of the knobby lobate material and the rest of the knobby lobate material in the crater center, leading us to hypothesize that this part of the unit was formed when part of the extensive deposit of knobby lobate material flowed from the crater center over the terraces in the direction of the crater rim.

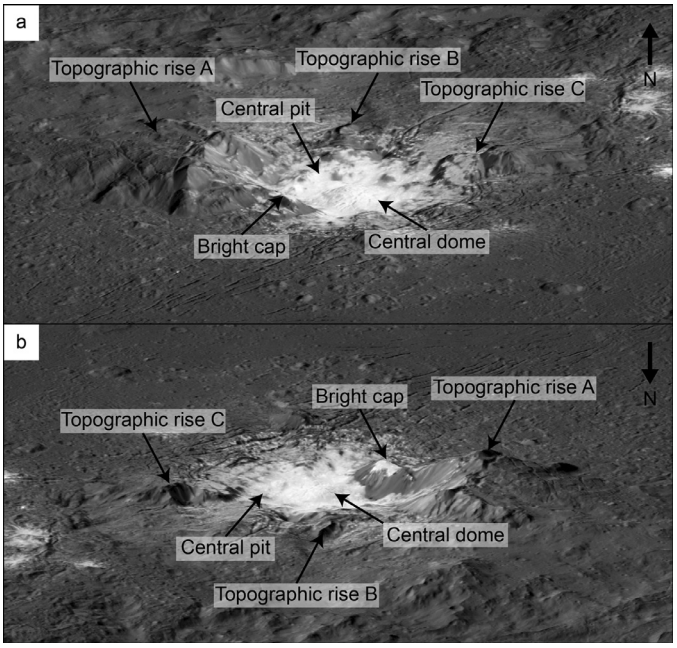

Fig. 8. The central pit, central dome, topographic rises and bright cap of material in perspective views (a) from the south to the north and (b) from the north to the south. The perspective views have no vertical exaggeration and were made by David P. O'Brien (Planetary Science Institute).

knobby lobate material. When there is a clearly observable boundary we map a certain contact and when it is difficult to pinpoint the exact contact between the outer, diffuse edge of Cerealia Facula and the units it superposes, we map the boundary using an approximate contact. In one instance the bright material forms a cap on the top of an otherwise dark hill on the southwestern margin of the central pit (Fig. 8). A dome is located within the center of the central pit, and is entirely covered by the Cerealia Facula bright material. This dome is capped by a radiating set of fractures (see Section 3.5). The central pit is surrounded by concentric fractures, which cross-cut the outer, diffuse edge of Cerealia Facula and are proposed to form during the formation/collapse of the central pit (Buczkowski et al., 2018b; Schenk et al., 2018). The morphology of Occator crater is discussed in context with central pit craters across the solar system in Schenk et al. (2018).

The Vinalia Faculae are a cluster of roughly circular diffuse bright material deposits that are located to the east of the Cerealia Facula (Fig. 5h). Their diffuse morphology is reminiscent of the discontinuous halo of diffuse material that makes up the outer edge of Cerealia Facula. Vent-like structures are visible in the centers of some of the Vinalia Faculae deposits (Ruesch et al., 2018; Nathues et al., 2018). The Vinalia Faculae superpose the hummocky lobate material and because an exact contact cannot be pinpointed between these two units, we map the boundary using an approximate contact. A set of fractures cross-cut the hummocky lobate material and are associated with the Vinalia Faculae (Buczkowski et al., 2018b). Two small impact craters (a few hundreds of meters in diameter) and their dark ejecta superpose the eastern side of the Vinalia Faculae (see Section 3.2.1).

Interpretations: We interpret that the outer edge of Cerealia Facula was emplaced before the formation of the central pit, because the concentric fractures, which likely formed during pit collapse, cross-cut the outer edge of Cerealia Facula. The cap of bright material could have been stranded on the otherwise dark hill during to the collapse of the central pit. There is no cross-cutting relationship observed between the majority of Cerealia Facula and the concentric fractures. Thus, the majority of Cerealia Facula could have formed, been modified and/or continued to form after the formation of the concentric fractures/central pit. The diffuse morphology of the Vinalia Faculae and their vent-like central structures suggest they were formed by a ballistic process (Ruesch et al., 2018; Quick et al., 2018; Nathues et al., 2018). The Dawn team's synthesized interpretation of the formation mechanism of Cerealia Facula, the central pit, the central dome and the Vinalia Faculae are presented in Scully et al., (2018a).

3.2.8. Talus material, dark talus material

Observations: This unit occupies Occator's steeply sloping walls (~30–40°) and originates from the crater rim (Fig. 5i). The unit has a smooth surface texture and contains individual lobes of material that appear to originate from outcrops along the crater rim and cascade down the crater walls. This unit superposes the crater terrace material, dark crater terrace material, smooth lobate material, knobby lobate material and dark knobby lobate material. We map certain contacts between this unit and the units it superposes. There are dramatic small-scale variations in the brightness of both the talus material and dark talus material on the scales of tens to hundreds of meters, because distinctly dark lobes of material are often adjacent to distinctly bright lobes of material. However, in general the dark talus material sub-unit is distinctly dark (pixel value: 0.01–0.05) in the photometrically corrected data, in comparison to the generally intermediate brightness of the talus material (pixel value: 0.05–0.06). The exact location of the boundary between the talus material and dark talus material is not visible in the photometrically corrected data, and thus we map it with an approximate contact.

Interpretations: We interpret that this unit formed as materials of varying brightness cascaded from outcrops on the crater rims down the crater walls. Thus, it is a mass-wasting deposit. Sometimes brighter and darker lobes of talus material are juxtaposed on scales of tens to a few hundreds of meters, indicating that materials of contrasting brightness can be juxtaposed on relatively small scales within Ceres' subsurface. The superposition relationships indicate that this is one of the youngest units within Occator crater. It is likely that instabilities in the talus material and/or seismic shaking from the formation of nearby, younger impact craters triggered the mass wasting that formed this unit.

3.3. Point features in the geologic map of Occator crater

Using the bright spot point feature, we map regions that are <500 m in size and are distinctly bright in the photometrically corrected data (pixel value > 0.06). These bright spots are spread throughout the interior and ejecta of Occator crater, but they tend to cluster around the Cerealia Facula and around Occator's rim (Fig. 4). Some bright spots are roughly circular and cross-cut many different types of geologic units (Fig. 9a). Within the centers of the larger of these roughly circular bright spots are impact craters from ~100 m to a few kilometers in diameter (Fig. 9b). The brightest of the roughly circular bright spots superpose Cerealia Facula (Fig. 9b). Bright spots also take the form of outcrops that occur on slopes, such as the walls of Occator and the eastern face of the largest topographic rise adjacent to the central pit (Fig. 9c) (see Section 3.5). Bright elongate lobes originate from these bright outcrops.

We interpret that the roughly circular bright spots are small impact craters and their ejecta blankets, which are composed of bright material that was excavated from Ceres' subsurface by the small impact craters. While some of the larger roughly circular bright spots contain impact craters a few hundreds of meters in diameter, impact craters that are smaller than the resolution limit of our data (less than ~60–70 m in diameter) are likely within the centers of the smaller roughly circular bright spots. The roughly

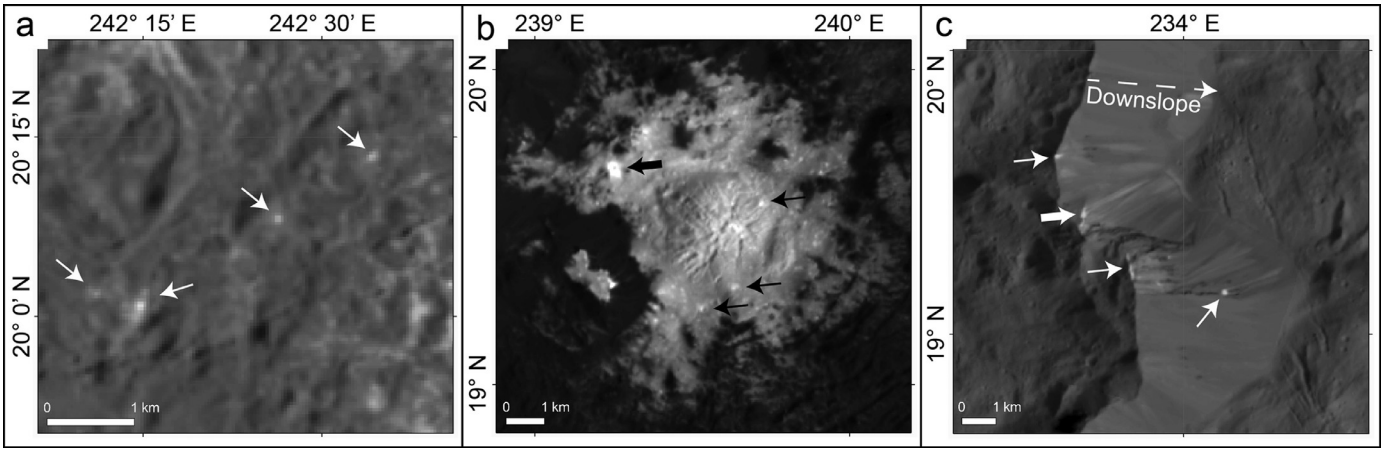

Fig. 9. The different types of bright spots in Occator crater. (a) Four roughly circular bright spots (indicated by white arrows). These are likely the bright ejecta deposits of impact craters that are smaller than the resolution limit of our data (less than ~60–70 m in diameter). (b) Examples of bright spots within Cerealia Facula are indicated by black arrows. The thick black arrow indicates a bright spot that is a ~140 m diameter impact crater surrounded by its bright ejecta blanket (also see Fig. 12 in Nathues et al., 2018). (c) White arrows indicate four examples of bright spots that are outcrops that occur on slopes. These outcrops are often the source regions for bright, elongate mass wasting deposits. A particularly distinctive bright, elongate mass wasting deposit is indicated by the thick white arrow.

circular bright spots that superpose the Cerealia Facula are small impact craters that excavated bright ejecta from below the surface of the Cerealia Facula. Thus, this indicates that the Cerealia Facula material is even brighter at depth and that the current surface of the Cerealia Facula may have been somewhat darkened by mixing with darker background material and perhaps by space weathering (Bu et al., 2018; Palomba et al., 2018; Stein et al., 2018). The bright spots that occur on slopes are outcrops of bright material that are the source regions for bright, elongate mass wasting deposits.

3.4. Linear features in the geologic map of Occator crater

We map the rims of impact craters that are > 5 km in diameter and classify them into two groups: raised rim impact craters have rims with a fresh and sharp appearance while degraded rim impact craters have rims with a comparatively rounded appearance. The remaining linear features within and surrounding Occator crater have been studied in detail by Buczkowski et al. (2016), Buczkowski et al. (2018a), Buczkowski et al. (2018b), Scully et al. (2017) and Scully et al. (2018c). Here we summarize the results of these aforementioned publications.

Scully et al. (2018c) and Scully et al. (2017) interpret that the impact crater chains and furrows surrounding Occator are secondary crater chains that formed as material ejected during Occator's formation bounced across and scoured the surrounding terrain (Fig. 10). Impact crater chains form when the ejected material impacts and bounces across the surface, while furrows form when the ejected material scours the surface. Many of the impact crater chains and furrows surrounding Occator are radial to the crater. However, in particular in the northeast and northwest, there are furrows and some impact crater chains that are not radial to the crater. Non-radial grooves/furrows are interpreted to be carved by the scour of debris ejected from the initial touchdown of an oblique crater-forming impactor uprange of the crater center (Schultz and Crawford, 2016). These non-radial grooves/furrows form prior to the deposition of radial secondary crater chains (Schultz and Crawford, 2016). Thus, we propose that Occator's non-radial furrows and impact crater chains are from the early ejection of material from the first touchdown of the impactor, while the radial impact crater chains and furrows formed during a later stage of ejection of material.

There is also a set of secondary crater chains called the Junina Catenae, which are oriented approximately east–west and are cross-cut by the northern part of Occator crater and its ejecta (Fig. 10). Only the portion of the Junina Catenae that are superposed by Occator and its ejecta are shown in our map (Fig. 3). The Junina Catenae are interpreted to derive from the formation of the Urvara and Yalode impact craters (Scully et al., 2018c; Scully et al., 2017).

There are numerous pit chains and grooves within Occator crater and within the ejecta blanket, which are interpreted as fractures formed by a variety of processes (Fig. 10) (Buczkowski et al., 2018b). For example, the pit chains and grooves that are concentric to the central pit are interpreted as fractures that formed during the collapse of the central pit (Buczkowski et al., 2018b; Schenk et al., 2018). These fractures cross-cut the hummocky crater floor material, the knobby lobate material and the outer edge of Cerealia Facula. There is also an additional set of fractures, which are associated with the Vinalia Faculae and cross-cut the hummocky lobate material (Buczkowski et al., 2018b).

The southern portion of Occator's ejecta blanket cross-cuts one of the Samhain Catenae, which are pit chains and grooves that are interpreted to be the surface expression of subsurface faults or fractures (Fig. 10) (Buczkowski et al., 2016; Scully et al., 2018c; Scully et al., 2017). Grooves form when chains of pits elongate and merge. Only the portion of the Samhain Catenae that are superposed by Occator and its ejecta are shown in our map (Fig. 3).

3.5. Topographic features in the geologic map of Occator crater

There are portions of Occator's interior that have a distinct topographic expression, but do not form a separate geologic unit. The first such region is the central pit (Fig. 8). Using the depression symbol, we map the break in slope between the edge of this central pit and the surrounding surface. The central pit is roughly circular, has an average diameter of ~8–9 km and is ~800 m deep. Within the central pit there is a central dome that is also roughly circular, has an average diameter of ~3.5 km and is a maximum of ~700 m high (Fig. 8). We map the break in slope around the base of the central dome using the dome symbol.

There are three topographic rises within the hummocky crater floor material, which are located adjacent to the western, northern and eastern sides of the central pit (Fig. 8). These topographic rises may be the remnants of an initial central peak. See Schenk et al. (2018) for further discussion of Occator in the context of central pit and central peak craters throughout the Solar

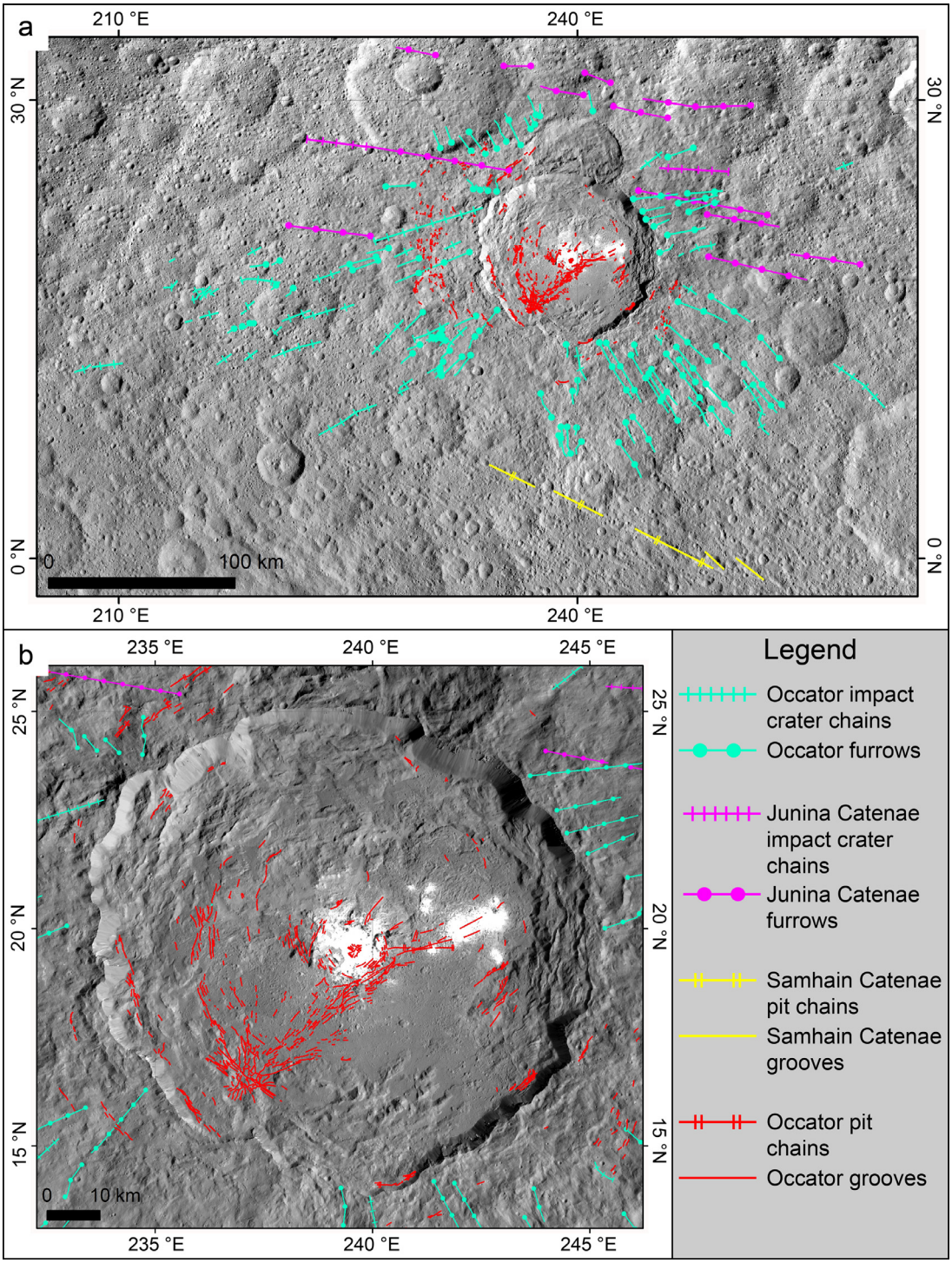

Fig. 10. The impact-derived and tectonically-derived linear features in (a) the entire map area and (b) the interior of Occator crater. Cyan lines are impact crater chains and furrows, which make up secondary crater chains that are derived from the material ejected during Occator's formation. Pink lines are impact crater chains and furrows that make up the Junina Catenae, which are secondary crater chains that derive from the formation of the Urvara and Yalode impact craters. Yellow lines are the Samhain Catenae pit chains and grooves, which are interpreted to be the surface expression of subsurface faults or fractures. Red lines are the pit chains and grooves within Occator crater and its ejecta blanket, which are interpreted as fractures. Only the portions of the Junina Catenae and Samhain Catenae that are superposed by Occator and its ejecta are shown in this map, in Fig. 3 and in Fig. 4. The map is displayed with an equirectangular projection, in which the scale bar is valid at the equator and the distortion increases towards the poles.(For interpretation of the references to color in this figure legend, the reader is referred to the web version of this article).

System. Topographic rise A, to the west, is ~9 km × ~11 km around its base. It rises a maximum height of ~1 km from the surrounding terrain to its highest point. Topographic rise B, to the north, is ~2 km × ~4 km around its base. It rises a maximum height of ~400 m from the surrounding terrain to its highest point. Topographic rise C, to the east, is ~4 km × ~7 km around its base. It rises a maximum height of ~700 m from the surrounding terrain to its highest point. We map the break in slope around the bases of A, B, and C using the topographic rise or hill symbol. The central dome, central pit and surrounding topographic rises are discussed further in Section 4.2.

4. Discussion

4.1. Insights derived from geologic mapping

4.1.1. Direction and angle of Occator-forming impactor

Asymmetric ejecta blankets are consistent with oblique impactors, and in the case of impactors that impacted at an angle of ~45°, the ejecta in the downrange direction is thicker and more extensive than the uprange ejecta. Moreover, the uprange ejecta becomes almost non-existent when the impact angle reaches ~30°, and the resulting impact craters become clearly elliptical at impact angles of ~10° (e.g. Melosh, 2011). As observed in Section 3.2.1, the majority of the ejecta surrounding Occator crater is located to the southeast (Fig. 3a): the average distance from the crater rim to the edge of the southeasterly ejecta is ~130 km, while the average distance from the crater rim to the edge of the northwesterly ejecta is ~70 km. Whilst Occator's ejecta is asymmetric, the crater itself has a consistent diameter of ~92 km. Therefore, these observations are consistent with the Occator-forming impactor originating from the northwest with an impact angle of ~30–45°. A northwestern origination for the Occator-forming impactor is consistent with the location of the non-radial furrows and impact crater chains to the northeast and northwest of Occator (see Section 3.4), which indicate that the uprange direction is roughly to the north. In addition, such non-radial furrows and impact crater chains are thought to form during oblique impacts of ~15–30° (Schultz and Crawford, 2016), indicating that the Occator-forming impactor had an impact angle closer to the ~30° end of the ~30–45° range.

4.1.2. Thicknesses of the faculae

We previously described two small impact craters and their dark ejecta blankets, which superpose the eastern part of the Vinalia Faculae (see Sections 3.2.1 and 3.2.7) (Fig. 5h). We interpret that these impact craters excavated through the Vinalia Faculae to the underlying darker material. The northernmost crater is ~250 m in diameter and the southernmost crater is ~500 m in diameter. Both are simple craters, because the Cerean simple to complex transition diameter occurs at ~7.5–12 km (Hiesinger et al., 2016). Using the excavation depth value of a terrestrial simple crater, Barringer crater (>0.08 times the final rim diameter) (Shoemaker, 1963; Osinski et al., 2011), we find that these impact craters likely excavated material from depths of approximately >20 m and approximately >40 m, respectively, within Ceres' subsurface. Thus, in this particular region, the Vinalia Faculae deposits are a maximum of approximately >20–40 m thick. Nathues et al. (2017) independently estimate that the Vinalia Faculae are a few meters thick.

There are two small regions (~1 km across) of hummocky crater floor material within Cerealia Facula (Fig. 5g), which are similar in scale and pattern to the small dark craters that superpose the Vinalia Faculae. However, instead of being the dark ejecta blankets of impact craters that excavated through Cerealia Facula, these regions are likely mounds around which the faculae-forming materials flowed (Schenk et al., 2018). Thus, because there are no recognizable small impact craters and dark ejecta blankets that superpose Cerealia Facula, we cannot estimate the upper bound of Cerealia Facula's thickness. However, there are the bright spots that occur on Cerealia Facula, which we previously interpreted to be bright ejecta excavated by small impact craters (Fig. 9b) (see Section 3.3). Many of the impact craters that we propose to be at the centers of these bright ejecta blankets are below the resolution limit of our data (less than ~60–70 m in diameter). Fortunately, there is one impact crater that is unambiguously resolved, which is ~140 m in diameter (Fig. 9b; also see Fig. 12 in Nathues et al., 2018). Using the excavation depth value of Barringer crater (Shoemaker, 1963; Osinski et al., 2011), we find that this impact crater likely excavated material from approximately >11 m below the surface. Thus, Cerealia Facula is approximately > 11 m thick in this region.

4.1.3. Nature of the lobate materials

The lobate materials have been previously interpreted as impact melt, or as mass wasting deposits, or as cryovolcanic flows (e.g. Jaumann et al., 2017; Krohn et al., 2016; Nathues et al., 2017; Schenk et al., 2016). As described in Sections 3.2.4–3.2.6, in our geologic mapping we find that the lobate materials are located in: (i) an extensive deposit in the southern and eastern crater floor and (ii) in separate, pond-like deposits (Fig. 7a). All but one of the regions of lobate material (the dark knobby lobate material) lack an origination point. The dark knobby lobate material appears to originate near the crater wall. However, the superposing dark talus material obscures the exact origination point of the dark knobby lobate material.

The lobate materials superpose, and appear to have flowed out onto, the hummocky crater floor material and crater terrace material. For example, the knobby material in the southeast of the crater appears to have flowed over the middle of a set of originally connected terraces (Fig. 7b) (see Section 3.2.5). We propose that the lobate materials are impact melt that was formed by the Occator-forming impact. This is consistent with Schenk et al. (2018) and references therein, and with the geomorphological characteristics of the lobate materials observed in our map: their location within an impact crater, the occurrence of separate, pond-like deposits of lobate material at different elevations throughout the crater, and the lack of clear origination points for the lobate materials. We interpret that the melting occurred during/immediately after the Occator-forming impact. The smooth and knobby lobate materials grade into one another, which indicates that they are not completely separate units. We interpret that their textural differences are most likely to be due to blocks greater than the resolution of the data (>35 m) being present in the knobby lobate material, and not within the smooth lobate material (see Sections 3.2.4–3.2.5). The hummocky surface texture of the hummocky lobate material, and its higher elevation than the smooth and knobby lobate materials, are suggested to be due to post-emplacement inflation, where the surface cools but the interior liquid volume increases via high effusion rates and sustained injection, possibly from a reservoir of material underlying Occator crater (see Buczkowski et al., 2018b for full discussion). Thus, the hummocky lobate material may have originally had a surface texture similar to the smooth and/or knobby lobate materials, and was later modified to become hummocky.

Model ages derived from crater counts are a suitable test of our geomorphological-based interpretation of the lobate materials. If the lobate materials are impact melt, the lobate materials should have similar model ages to Occator's ejecta. However, if later processes, such as mass wasting or cryovolcanic flows formed the lobate materials, they should have younger model ages than Occator's ejecta. Nathues et al. (2018) interpret the lobate materials as a debris avalanche deposit originating from mass wasting along the southeastern crater wall. Model ages derived by Nathues et al. (2017) and references therein indicate that the lobate materials are significantly younger than the formation age of Occator: ~6.9 ± 0.9 Ma versus ~34 ± 2 Ma, respectively. These model ages are consistent with the lobate materials being formed by a later process, and not impact melt. However, Neesemann et al. (2018) identified an ENE-WSW trending elongated secondary crater cluster that cross-cuts a large part of Occator's southern ejecta and the southern part of the crater terrace material. They argue that including this crater cluster in counts results in erroneously old model ages, and omit it from their analysis. Without the inclusion of this crater cluster, Neesemann et al. (2018) find almost identical ages for Occator's

ejecta, 21.91 ± 0.68 Ma, and the lobate material, 19.18 ± 2.00 Ma. Therefore, these model ages are consistent with the lobate materials being impact melt.

Another test of our geomorphological-based interpretation of the lobate materials is to compare the volume of the lobate materials to the volume of melted material predicted to form during the Occator-forming impact (Bowling et al., 2018). If the volume of the lobate materials is less than the volume of melted material, the lobate materials can be an impact melt. However, if the volume of the lobate materials is greater than the volume of the melted material, the lobate materials cannot have formed in a solely impact-driven process.

We estimate the volume of the lobate materials by measuring the total area of the lobate materials in our geologic map: ~2141 km^2. We make profiles of the Occator shape models at various locations across the crater, in order to estimate the average thickness of the lobate materials. Consistent with Buczkowski et al. (2018b), we find that the hummocky lobate material is ~200 m higher than the surrounding materials. However, much of this height is likely due to post-emplacement modification (Buczkowski et al., 2018b) and is thus not representative of the initial thickness of the lobate material. Additionally, the profiles of the smooth and knobby lobate materials do not allow for the estimation of conclusive thicknesses. Therefore, we use a variety of assumed thicknesses to estimate the volume of the lobate materials. Assuming that the average thickness of the lobate materials is ~1 m, ~10 m, ~100 m or ~1 km, we derive volumes of ~2 km^3, ~20 km^3, ~200 km^3 or ~2000 km^3, respectively. Average thicknesses of ~1 m or ~1 km are likely unrealistically thin or unrealistically thick. Thus, we propose that the intermediate volumes (~20–200 km^3) are closer to the real volume of the lobate materials.

Impact modeling predicts that while the Occator-forming impact would not be energetic enough to melt silicates and salts, approximately 1000 km^3 of target material would be heated above the melting point of water (>273 K) during Occator's formation (Bowling et al., 2018), which is much greater than our estimate of the volume of the lobate materials (~20–200 km^3). In this scenario, a slurry of impact-melted water mixed with particulates and boulders of unmelted silicates and salts would be formed. Thus, we propose that while mobile during the early stages of Occator's evolution, while the crater was still relatively warm, this impact slurry flowed around the crater interior before solidifying to form the lobate materials.

4.2. Geologic history

Based on the observations and interpretations derived from our geologic map, we place the geologic units in stratigraphic order (Fig. 11) and propose the following geologic history for Occator crater:

- The Samhain Catenae pit chains and Junina Catenae secondary crater chains are pre-existing in the region that will later host Occator crater.
- The Occator-forming impactor originates from the northwest with an impact angle of ~30–45°, perhaps closer to ~30° When it impacts the surface, ejecta is thrown in all directions, with the majority being thrown in the downrange direction. The majority of the ejecta has an intermediate brightness. On the eastern side, darker ejecta is excavated from deeper within Ceres and superposes the intermediate brightness ejecta. The source material for the dark ejecta may have been more common within the eastern subsurface or may have been more deeply buried within the western subsurface. See Nathues et al. (2018) and Raponi et al. (2018) for additional discussion of Occator's dark ejecta. Secondary crater chains are also formed around Occator crater, as material ejected during the formation of the crater impacts, bounces across and scours the surface: non-radial features form early, due to the first touchdown of the impactor, while radial features form during a later stage of ejection of material.
- Shortly after the initial impact, crater-wall collapse and mass wasting leads to the formation of crater terrace material and hummocky crater floor material within the interior of Occator. The convergence of sets of collapsing terraces form ~90° bends in the crater rim.
- The energy derived from the impactor heats and melts some of the target material. This slurry of impact-melted water and unmelted silicate/salt blocks would be mobile for a geologically short timescale after the impact (approximately less than a few millions of years). See Bowling et al. (2018) for additional discussion about impact-derived energy.
- While mobile, the lobate materials superpose the crater terrace material and hummocky crater floor material before solidifying in place. A large region of lobate material concentrates in the southern and eastern crater floor, and smaller ponds also form throughout the crater floor at different elevations. It is likely that knobby and smooth surface textures form if the lobate material entrain or does not entrain blocks. See Schenk et al. (2018) and Nathues et al. (2018) for additional discussion of the lobate material.
- The outer edge of Cerealia Facula is emplaced prior to the formation of the central pit, because the concentric fractures, which likely formed during pit collapse (Buczkowski et al., 2018b; Schenk et al., 2018), cross-cut the outer edge of Cerealia Facula. On account of the concentric fractures cross-cutting the knobby lobate material, the pit collapse must also have happened after the solidification of at least part of the knobby lobate material. A portion of Cerealia Facula may also have been

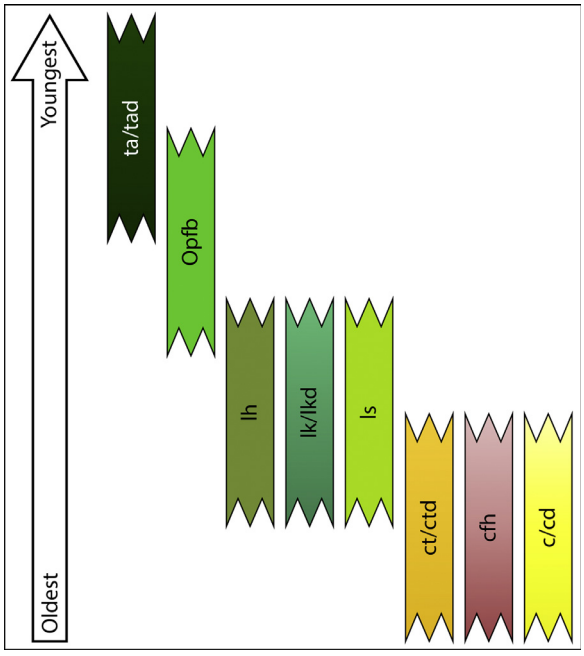

Fig. 11. Correlation of Map Units, which illustrates the stratigraphic order into which we place the mapped geologic units. The oldest units are at the bottom and the youngest units are at the top. c/cd is the crater material/dark crater material. cfh is the hummocky crater floor material. ct/ctd is the crater terrace material/dark crater terrace material. ls is the smooth lobate material. lk/lkd is the knobby lobate material/dark knobby lobate material. lh is the hummocky lobate material. Opfb is the bright Occator pit/fracture material. ta/tad is the talus material/dark talus material.

left stranded on the top of a dark hill during the collapse of the central pit. See Buczkowski et al. (2018b) for additional discussion of the fractures within Occator.

- The central pit and its concentric fractures form. Schenk et al. (2018) suggest that the central pit formed via the 'melted uplift model', where a liquid water central uplift drained into fractures, leaving behind a central pit. The majority of Cerealia Facula (approximately >11 m thick), which is not cross-cut by the concentric fractures, may have been formed, modified and/or continued to form after the formation of the central pit. Schenk et al. (2018) propose that the majority of Cerealia Facula formed as brines flowed out of fractures along the pit walls, eventually accumulating in the central region before the loss of the liquid portion left behind a bright, salty residue. The faculae-forming brines could also have been emplaced on the surface via salt-rich water fountaining (Ruesch et al., 2018). There are lines of evidence that indicate these brines could be entirely due to the Occator-forming impact, but there are also lines of evidence that suggest an endogenic component to their formation (see Scully et al., 2018a for a full discussion).
- The distinctly hummocky texture of the northeastern part of the extensive deposit of lobate material is suggested to be due to post-emplacement inflation (Buczkowski et al., 2018b). There are no clearly defined stratigraphic relations to indicate whether this occurred simultaneously with, before, or after the formation of the Cerealia Facula and the central pit.
- The Vinalia Faculae (a maximum of approximately >20–40 m thick) are emplaced, superposing the hummocky lobate materials. The diffuse nature of the Vinalia Faculae suggests that they were formed via a salt-rich water fountaining mechanism (Ruesch et al., 2018), which can easily occur in Ceres' surface conditions (Quick et al., 2018). The uplift of the hummocky lobate material is proposed to form fractures (Buczkowski et al., 2018b), which allowed the Vinalia Faculae-forming materials to reach the surface (see Scully et al., 2018a for a full discussion).
- The central dome forms within the Cerealia Facula (e.g. Quick et al., 2018; Ruesch et al., 2018; Schenk et al., 2018). As it forms, the bright Cerealia Facula material on top of the dome is fractured in a radial pattern. There are no clearly defined stratigraphic relations to indicate whether the dome formed before, after or contemporaneously with the Vinalia Faculae (see Scully et al., 2018a for a full discussion).
- Geologically recent mass wasting events form talus material, mostly on the walls of Occator crater. This mass wasting may result from instabilities in the talus material and/or seismic shaking from the formation of nearby, younger impact craters. Some of this mass wasting exposes bright material, which form bright, elongate mass wasting deposits.
- Geologically recent impacts form small impact craters (~100 m to a few kilometers in diameter) throughout Occator and its ejecta, which excavate and expose bright material from the subsurface. The brightest material is excavated on Cerealia Facula. See Bu et al. (2018), Palomba et al. (2018) and Stein et al. (2018) for additional discussion of darkening of the faculae materials. Comparatively darker material is excavated from below, and deposited on top of, the Vinalia Faculae by small impact craters. One of these dark ejecta blankets superposes the fractures associated with the Vinalia Faculae, indicating that the impact occurred after the formation the fractures.

5. Conclusions

The aim of this work is to use focused, detailed geologic mapping of the interior of Occator crater and its ejecta to provide new insights into Occator and its faculae. These insights are one group of inputs that will be used to identify the driving forces behind the formation of Occator and its faculae. These inputs, and inputs from all of the studies in this special issue, will be synthesized together in Scully et al., (2018a), with the aim of leading to a new understanding of the processes and conditions in Ceres' past, and potentially in its present. The main inputs derived from this study are as follows:

1. The crater terrace material, hummocky crater floor material and talus material within Occator are also found within other complex craters in the region. The geologic units of Occator crater that make it unique are the Cerealia Facula, the Vinalia Faculae and the extensive, well-preserved lobate materials.
2. On the basis of geomorphological evidence derived from our geologic map and on impact modeling (Bowling et al., 2018), we propose that the lobate materials are a slurry of impact-melted and non-impact-melted target material that flowed around the crater interior prior to solidifying. This interpretation is consistent with Schenk et al. (2018) and one set of model ages of Occator (Neesemann et al., 2018). The lobate materials are discussed further in the synthesis of this special issue (Scully et al., 2018a).
3. At least part of the knobby lobate material and the outer edge of the Cerealia Facula were emplaced prior to the formation of the central pit. The majority of Cerealia Facula may have formed, continued to form and/or have been modified after the formation of the central pit.
4. We identify one set of stratigraphic relations within the Cerealia Facula region and another set stratigraphic relations within the Vinalia Faculae region. However, our mapping does not identify any clearly defined stratigraphic relations between these two sets. Set #1: The outer edge of the Cerealia Facula formed prior to the central pit. After the formation of the central pit, the dome formed and the majority of the Cerealia Facula may have formed, continued to form and/or have been modified. Set #2: The Vinalia Faculae formed after the hummocky lobate material.
5. The diffuse morphology of the Vinalia Faculae is reminiscent of the Cerealia Facula's discontinuous outer edge of diffuse material. This suggests that the Cerealia Facula may have initially been emplaced in similar process to the Vinalia Faculae. It is possible that the majority of the present-day Cerealia Facula is morphologically dissimilar to the Vinalia Faculae because of the continued formation/modification of the Cerealia Facula and the formation of the central dome.
6. The Cerealia Facula material that is underneath the surface is even brighter than the surficial Cerealia Facula material, as indicated by small impact craters and their ejecta blankets that superpose the Cerealia Facula. Thus, the surficial Cerealia Facula material has likely somewhat darkened since it was initially emplaced.

Acknowledgments

Part of the research was carried out at the Jet Propulsion Laboratory, California Institute of Technology, under a contract with the National Aeronautics and Space Administration. We thank the Dawn Flight Team at JPL for the development, cruise, orbital insertion and operations of the Dawn spacecraft at Ceres. We thank the instrument teams at the Max Planck Institute, German Aerospace Center (DLR), Italian National Institute for Astrophysics (INAF) and Planetary Science Institute (PSI) for the acquisition and processing of Dawn data. The data upon which we base our mapping are available on the PDS Small Bodies Node website at https://sbn.psi.edu/pds/resource/dwncfc2.html.

Supplementary materials

Supplementary material associated with this article can be found, in the online version, at doi:10.1016/j.icarus.2018.04.014.

References

Ammannito, E., et al., 2016. Distribution of phyllosilicates on the surface of Ceres. Science 353 (6303) aaf4279, 1–5.

Bland, M.T., et al., 2016. Composition and structure of the shallow subsurface of Ceres as revealed by crater morphology. Nat. Geosci. 9, 538–542.

Bowling, T., et al., 2018. Post-impact thermal structure and cooling timescales of occator crater on asteroid 1 Ceres. Icarus this issue.

Bu, C., et al., 2018. Stability of hydrated carbonates on Ceres. Icarus this issue.

Buczkowski, D.L., et al., 2018a. The geology of the Occator quadrangle of dwarf planet Ceres: floor-fractured craters and other geomorphic evidence of cryomagmatism. Icarus in press.

Buczkowski, D.L., et al., 2018b. Tectonic analysis of fracturing associated with Occator crater. Icarus this issue.

Buczkowski, D.L., et al., 2016. The geomorphology of ceres. Science 353 (6303) aaf4332, 1–8.

Carrozzo, F.G., et al., 2018. Nature, formation and distribution of carbonates on Ceres. Sci. Adv. 4 (3), e1701645.

Combe, J.-P., et al., 2016. Detection of local H_2O exposed at the surface of Ceres. Science 353 (6303) aaf3010, 1–6.

De Sanctis, M.C., et al., 2016. Bright carbonate deposits as evidence of aqueous alteration on Ceres. Nature 536, 54–57.

De Sanctis, M.C., et al., 2015. Ammoniated phyllosilicates with a likely outer solar system origin on (1) Ceres. Nature 528, 241–243.

De Sanctis, M.C., et al., 2011. The VIR spectrometer. Space Sci. Rev. 163, 329–369.

Ermakov, A.I., et al., 2017a. Constraints on Ceres' internal structure and evolution from its shape and gravity measured by the Dawn spacecraft. J. Geophys. Res. 112 (11), 2267–2293.

Ermakov, A.I., et al., 2017b. Ceres' obliquity history and its implications for the permanently shadowed regions. Geophys. Res. Lett. 44, 2652–2661.

Federal Geographic Data Committee [prepared for the Federal Geographic Data Committee by the U.S. geological Survey], 2006. FGDC Digital Cartographic Standard for Geologic Map Symbolization. Federal Geographic Data Committee. p. 290.

Fu, R.R., et al., 2017. The interior structure of Ceres as revealed by surface topography. Earth Planet. Sci. Lett. 476, 153–164.

Hiesinger, H., et al., 2016. Cratering on Ceres: implications for its crust and evolution. Science 353 (6303) aaf4759, 1–8.

Hughson, K.H.G., et al., 2018. The Ac-5 (Fejokoo) quadrangle of Ceres: geologic map and geomorphological evidence for ground ice mediated surface processes. Icarus in press.

Jaumann, R., et al., 2017. Topography and geomorphology of the interior of Occator crater on Ceres. Lunar and Planetary Science Conference XLVIII. Abstract 1440.

Konopliv, A.S., et al., 2011. The Dawn gravity investigation at Vesta and Ceres. Space Sci. Rev. 163, 461–486.

Krohn, K., et al., 2016. Cryogenic flow features on Ceres: implications for crater-related cryovolcanism. Geophys. Res. Lett. 43, 11994–12003.

Li, J.-Y., et al., 2016. Surface albedo and spectral variability of Ceres. Astrophys. J. Lett. 817, L22.

Longobardo, A., et al., 2018. Mineralogy of the Occator quadrangle. Icarus in press.

Marchi, S., et al., 2016. The missing large impact craters on Ceres. Nat. Commun. 7 (12257), 1–9.

Melosh, H.J., 2011. Planetary Surface Processes. Cambridge University Press, p. 245.

Nathues, A., et al., 2018. Occator crater in color at highest spatial resolution. Icarus this issue.

Nathues, A., et al., 2017. Evolution of Occator crater on (1) Ceres. Astron. J. 153 1–12.

Nathues, A., et al., 2015. Sublimation in bright spots on (1) Ceres. Nature 528, 237–240.

Neesemann, A., et al., 2018. The various ages of Occator crater, Ceres: results of a comprehensive synthesis approach. Icarus this issue.

Osinski, G.R., et al., 2011. Impact ejecta emplacement on terrestrial plants. Earth Planet. Sci. Lett. 310, 167–181.

Palomba, E., et al., 2018. Compositional differences among bright spots on the Ceres surface. Icarus this issue.

Park, R.S., et al., 2016. A partially differentiated interior for (1) Ceres deduced from its gravity field and shape. Nature 537, 515–517.

Platz, T., et al., 2016. Surface water-ice deposits in the northern shadowed regions of Ceres. Nat. Astron. 1, 0007.

Prettyman, T.H., et al., 2011. Dawn's gamma ray and neutron detector. Space Sci. Rev. 163, 371–459.

Preusker, F., et al., 2016. Dawn at Ceres – shape model and rotational state. Lunar and Planetary Science Conference XXXXVII Abstract 1954.

Quick, L.C., et al., 2018. A possible brine reservoir beneath Occator crater: thermal and compositional evolution and the formation of the Cerealia dome and the vinalia faculae. Icarus this issue.

Raponi, A., et al., 2018. Insight on the evolution of Occator crater on Ceres from the properties of carbonates, phyllosilicates, and chlorides. Icarus this issue.

Roatsch, T., et al., 2017. High-resolution Ceres low altitude mapping orbit atlas derived from dawn framing camera images. Planet. Space Sci. 140, 74–79.

Ruesch, O., et al., 2018. Bright carbonate surfaces on Ceres as remnants of salt-rich water fountains. Icarus this issue.

Ruesch, O., et al., 2016. Cryovolcanism on Ceres. Science 353 (6303) aaf4286, 1–8.

Russell, C.T., et al., 2016. Dawn arrives at Ceres: exploration of a small volatile-rich world. Science 353 (6303), 1008–1010.

Schenk, P.M., et al., 2018. The central pit and dome at cerealia facula bright deposit and floor deposits in occator crater, Ceres: morphology, comparisons and formation. Icarus this issue.

Schenk, P., et al., 2016. Impact cratering on the small planets Ceres and Vesta: S-C transitions, central pits and the origin of bright spots. Lunar and Planetary Science Conference XXXXVII Abstract 2697.

Schmidt, B.E., et al., 2017. Geomorphological evidence for ground ice on dwarf planet Ceres. Nat. Geosci. 10, 338–343.

Schorghofer, N., et al., 2016. The permanently shadowed regions of dwarf planet Ceres. Geophys. Res. Lett. 43, 6783–6789.

Schröder, S.E., et al., 2017. Resolved spectrophotometric properties of the Ceres surface from dawn framing camera images. Icarus 288, 201–225.

Schultz, P.H., Crawford, D.A., 2016. Origin and implications of non-radial imbrium sculpture on the Moon. Nature 535, 391–394.

Scully, J.E.C., et al., 2018a. Synthesis of the special issue: the formation and evolution of Ceres' occator crater. Icarus this issue.

Scully, J.E.C., et al., 2018b. Introduction to the special issue: the formation and evolution of Ceres' Occator crater. Icarus this issue.

Scully, J.E.C., et al., 2018c. Ezinu quadrangle on Ceres: a heavily cratered region with evidence for localized subsurface water ice and the context of Occator crater. Icarus in press.

Scully, J.E.C., et al., 2017. Evidence for the interior evolution of Ceres from geologic analysis of fractures. Geophys. Res. Lett. 44, 1–9.

Shoemaker, E.M., 1963. Impact mechanics at meteor crater. In: Middlehurst, B.M., Kuiper, G.P. (Eds.), The Moon, Meteorites and Comets. University of Chicago Press, Arizonalllinois, pp. 301–336.

Sierks, H., et al., 2011. The Dawn framing camera. Space Sci. Rev. 163, 263–327.

Sizemore, H.G., et al., 2017. Pitted terrains on (1) Ceres and implications for shallow subsurface volatile distribution. Geophys. Res. Lett. 44, 6570–6578.

Stein, N., et al., 2018. The formation and evolution of bright spots on Ceres. Icarus this issue.

Villarreal, M.N., et al., 2017. The dependence of the Cerean exosphere on solar energetic particle events. Astrophys. J. Lett. 838 1–5.

Williams, D.A., et al., 2018. Introduction: the geologic mapping of Ceres. Icarus in press.